SSC20-IX-09

A Miniaturized Green End-Burning Hybrid Propulsion System for CubeSats

Tyson K. Smith, Zachary Lewis, Kurt Olsen, A. Marc Bulcher
Space Dynamics Laboratory
North Logan, Utah 84341; 435-713-3099
Tyson.smith@sdl.usu.edu

Stephen A. Whitmore
Department of Mechanical and Aerospace Engineering, Utah State University
Logan, Utah 84322; 435-797-2951
stephen.whitmore@usu.edu

ABSTRACT

Conventional hybrid rocket motors with thrust levels greater than 5 N rely on forced convection within the boundary layer as the primary heat-transfer mechanism for fuel vaporization. For hybrid rockets with thrust levels less than 5 N, oxidizer mass flow levels are sufficiently small that the rate of convective heat transfer is significantly reduced, and *radiative heat transfer* dominates the fuel vaporization mechanism. Radiative heating is a potential concern when implementing traditional hybrid rocket core burn fuel grain designs for systems with low thrust levels adequate for small satellites and CubeSats. Radiative heating causes the system to be fuel rich leading to inefficient combustion and nozzle clogging. This paper presents a novel idea of using this radiative heating phenomenon in the design of a hybrid propulsion system suitable for CubeSats and small satellites. This paper presents the test results of two fuel grain designs, the first being an end burning design and the second a "sandwich" fuel grain design. ABS, PVC, Nylon-12 and acrylic known as PMMA were used as fuel and gaseous oxygen (GOX) was used as the oxidizer during this testing campaign. These propellants provide several advantages including: benign handling properties, simplified plumbing, and greater burn efficiency over traditional monopropellant hydrazine.

INTRODUCTION

Due to the lack of a reliable on-demand ignition system, hybrid rockets have never been seriously considered as a viable alternative for in-space propulsion. Fortunately, while researching various 3-D printable plastics as alternatives to legacy solid propellant binders like HTPB[1], the Propulsion Research Laboratory at Utah State University (PRL/USU) discovered certain printable materials like acrylonitrile butadiene styrene (ABS) allows the manufacture of a structural matrix with unique electrical breakdown properties. This discovery has allowed for the development of a unique on-demand ignition technology for hybrid rockets[2].

In the current CubeSat market, there does not exist a Commercial off the Shelf (COTS) propulsion system with flight heritage that has thrust levels greater than tens of millinewtons or specific impulse (I_{sp}) levels greater than 70 seconds. Electric propulsion systems provide very high I_{sp} but low thrust levels. The kinetic power per unit thrust surrounding electric propulsion systems are in the range of 10 – 100 W/mN[3] depending on selected type. These large power requirements, in addition to the low thrust of electric propulsion, either limit the mission CONOPS or extend the mission timeframe incurring addition financial expenditures. Cold gas propulsion systems are the opposite of electric systems in terms of performance with I_{sp} levels less than 70 seconds. The low I_{sp} of cold gas systems directly results in large form factors with poor volumetric performance.

The Space Dynamics Lab (SDL) is currently developing an advanced hybrid propulsion system that uses a safe, or "green," propellant to fill this technology gap.

The majority of hybrid rockets developed to date are traditional core-burning designs with significantly higher thrust levels than desired for small spacecraft. These designs also require a high length-to-diameter ratio, resulting in a form factor difficult to use in CubeSats or small satellites. This paper presents an end-burning design that addresses both the high thrust and form factor issues. The design presented has thrust levels ranging from 0.5-1 N and an overall chamber volume of approximately 1 U.

BACKGROUND

Current CubeSat Propulsion Market

As discussed in the introduction, there is a technology gap in the current CubeSat market. The gap exists in the "high" thrust and "moderate" specific impulse category. This category is traditionally filled by mono- or bi- propellants. Figure 1 shows the CubeSat propulsion market highlighting performance metrics for CubeSat systems with flight heritage. Flight heritage is defined here as a propulsion system that is on-orbit, but not necessarily fully functional. The CubeSat market is saturated with propulsion systems in some stage of development[6], Figure 1 only shows systems that have been on-orbit.

The technology gap in the CubeSat propulsion market leads to mission limitations including: 1) spacecraft attitude control difficulty due to centrally located thrusters, 2) low performing cold gas systems requiring large tanks, and 3) electric propulsion systems with large power requirements. These limitations make several mission types extremely difficult or, in some cases, unsupportable. Such missions include rendezvous, proximity operations, formation flying, and cluster management. A successful demonstration of a system in this technology gap would lead to a compact, highly efficient, and market disrupting propulsion system that that would enable CubeSats for use in critical and far-reaching missions. SDL's hybrid propulsion system aims to fill this gap.

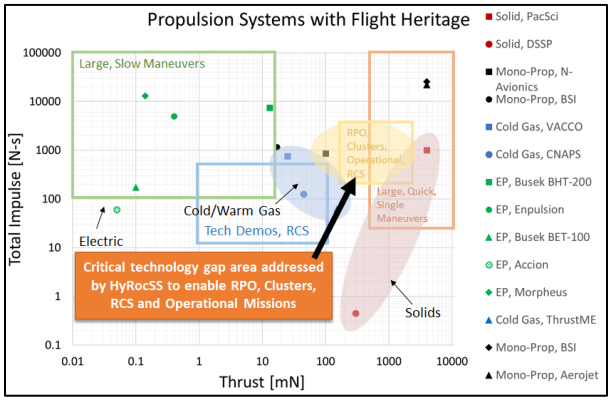

Figure 1. Current Market for CubeSat Propulsion Systems

Green Hybrid Propulsion System

Dedicated launches of Smallsats have increased each year since 2015[4] creating an industry need for a cost effective and high-performance propulsion system. Many satellite developers continue to use multi-million-dollar propulsion systems based on a propellant known as hydrazine[5]. The hybrid propulsion system in development at SDL aims to address this prohibitive cost requirement to allow more satellite developers an opportunity to incorporate propulsion into their design. Current efforts are being made by AFRL, NASA, and ECAPS to develop non-hydrazine "green" propellants. However, the costs are nearly identical to conventional hydrazine systems. The cost associated with these propulsion systems has led to many Smallsats launching with no propulsion; often restricting the mission CONOPS. In addition to the costs surrounding hydrazine and other "green" propellants are the hazards they pose to personnel.

Hybrid rockets typically consist of moderately benign gaseous or liquid oxidizer and an inert solid fuel. Hybrid rockets possess operational safety and handling advantages when compared to liquid and solid propellent systems. The U.S. Department of Transportation concluded that most hybrid rocket motor designs could be safely stored and operated without risk of explosion or detonation, potentially offering significantly lower operating and integration cost[8]. The inherent design safety of hybrid rockets increases the potential for rideshare[9] opportunities when compared to traditional monopropellant systems.

Disadvantages of Hybrid Rockets

In order for hybrid rockets to fill the technology gap discussed in the previous section there are two key disadvantages that must be addressed. The first is the difficulty surrounding motor ignition. A key reason why hybrid rockets are considered to be safe is due to the stability of their propellant. This stability makes hybrid rockets difficult to ignite. The hybrid rocket ignition source must provide sufficient heat to vaporize the solid fuel grain at the head end of the motor while simultaneously providing sufficient residual energy to overcome the activation energy of the propellants. Hybrid rockets typically use a pyrotechnic device called a "squib" that ignites a secondary solid propellant motor to initialize the combustion of the hybrid motor. These squibs are often susceptible to the hazards of electromagnetic radiation and can present a potential explosion hazard[11]. Also, pyrotechnic ignitors can only be fired once, thus limiting their application as an in-space propulsive device.

The second disadvantage is that the internal motor ballistics of hybrid combustion produce regression rates that are typically 25-30% lower when compared to solid fuel motors of the same thrust and impulse[10,11]. To make up for the lower regression rate, a higher oxidizer flow rate is required to maintain the same thrust level. This increases the systems oxidizer-to-fuel ratio (O/F) and ultimately results in poor mass impulse performance, erosive fuel burning, nozzle erosion, reduced motor duty cycles, potential combustion instability, and poorer

overall performance of the system. To overcome this O/F problem, hybrid rockets are traditionally designed with cylindrical fuel ports that have long length-to-diameter ratios. This high aspect ratio can result in poor volumetric efficiency and thus limit a hybrid motors application to a customarily volume constrained small satellite[12].

The SDL hybrid propulsion system addresses these two disadvantages. The solutions to these disadvantages are discussed in the following sections.

A Safe Restartable Ignition System

Whitmore et al[13] developed an arc-ignition system for traditional core burning hybrid motors that was adapted to SDLs hybrid end burning hybrid motor. They found that if a high voltage is applied across an insulator, then an electrical breakdown of the insulator will occur. The voltage where the insulator suffers electrical breakdown is referred to as breakdown voltage. This breakdown has been observed in solids, liquids, and gases[14].

The ignition system developed by Whitmore et al[13] consists of two electrodes embedded in an ABS fuel grain. The conduction paths terminate in electrodes that are flush with the combustion port surface and are exposed to the combustion chamber as shown in Figure 2. When these electrodes are separated by a small distance, the breakdown voltage between the two electrodes is too high to initiate direct metal to metal arcing, and thus an arc occurs along the surface of the fuel. The arc on the surface of the fuel causes local fuel vaporization to occur along the conduction path. They found that if an oxidizing agent was introduced to the combustion chamber prior to the time that fuel vaporization occurred there would exist a mixture of gaseous reactants and a source of activation energy in the combustion chamber. The energy release from the mixture of the vaporized fuel and the injected oxidizer causes rapid and self-sustaining combustion along the entire port surface. This innovation in safe, restartable hybrid technology alleviates the first disadvantage discussed in the previous section.

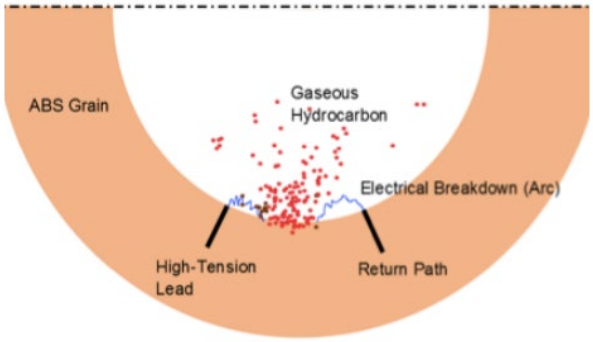

Figure 2. Arc Ignition Concept for a Core Burn Hybrid Rocket

An Argument for End Burning

Conventional hybrid rocket motors with thrust levels greater than 5 N rely on forced convection within the boundary layer as the primary heat transfer mechanism for fuel regression. Because of convective heat transfer, the rate of fuel regression is proportional to the oxidizer mass flux through the fuel port. As the fuel port burns radially outwards along the motors longitudinal axis, the rate of fuel regression results from oxidizer diffusion into the combustion layer between the inward blowing vaporized fuel and the axially flowing oxidizer. For a constant oxidizer mass flow, the associated mass flux and the fuel regression rate decrease with burn time. As the fuel port opens up, more surface burn area is exposed, and the resulting oxidizer-to-fuel ratio shifts during the burn from a balance between the fuel regression rate drop, and the increased surface burn area. Generally, the effects of forced convection tend to make hybrid motors burn from *rich-to-lean* over the burn lifetime[15].

For Hybrid rockets with thrust levels less than 5 N, oxidizer mass flow levels are sufficiently small that the rate of convective heat transfer is significantly reduced, and *radiative heat transfer* dominates the fuel regression mechanism[15]. Figure 3 shows how hybrid rockets with lower oxidizer mass flow levels are dominated by radiative heat transfer. This issue is associated with the miniaturization of hybrid rockets and has yet to be fully understood, but generally the fuel regression rate tends to grow with time. These small hybrid motors have exhibited a *lean-to-rich* burn behavior[15].

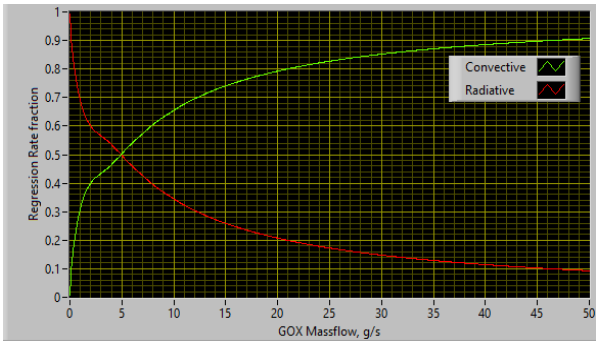

Figure 3. Regression rate for a hybrid motor as a function of oxidizer mass flow

This fuel-rich tendency leads to combustion inefficiencies in the scales necessary to achieve useful thrust levels for small satellites (<5 N). As a solution to provide constant fuel regression rate at these desired low thrust levels, the configuration was redesigned to be end-burning, resulting in a constant regression rate and oxidizer-to-fuel ratio throughout the burn lifetime. To our knowledge, the SDL/USU prototype is the first attempt at an end-burning hybrid thruster in the sub-Newton scale. This paper presents the design and testing results of the SDL hybrid propulsion system at thrust levels of 0.5 and 1 N.

SDL's hybrid propulsion system uses various plastics such as ABS, PMMA, PVC, and Nylon-12 as fuel and gaseous oxygen (GOX,) as the oxidizer. Future planned tests will include the use of high-density oxidizers such as hydrogen peroxide (H_2O_2) and nitrous oxide (N_2O). These propellants provide several advantages, including: benign handling properties, simplified plumbing, and greater characteristic velocities over traditional monopropellants.

EXPERIMENT SETUP

End-burn Design

USU/PRL discovered that a high voltage arc, when placed on the surface of Acrylonitrile butadiene styrene (ABS) plastic, resulted in fuel vaporization along the conduction path. This novel idea led to the development of several lab-weight thrusters varying in thrust from approximately 4 – 900 N[12]. In March of 2018, a 5 N system was successfully demonstrated on a suborbital sounding rocket. During this flight demonstration the system was fired 5 times with each firing lasting 5 seconds[7]. These successful tests led SDL and USU to begin investigating the opportunity to fill the current CubeSat market technology gap with this same technology by miniaturizing these ABS-based hybrid rockets to levels ≤5 N.

The end burn configuration, deemed the Augmented Swirling Injection (ASI) end burn motor, was designed to increase the flow of oxidizer across the fuel surface and to maintain a constant O/F ratio. The combustion chamber is located at the end of the fuel grain, and lies in between the fuel grain and the nozzle. The electrodes run through the length of the fuel grain and terminate flush with the combustion chamber surface allowing for fuel vaporization. The oxidizer is injected at four points to induce a swirling internal flow, effectively increasing the mixing of the oxidizer with the vaporized fuel. A side view of the end burn design is shown in Figure 4.

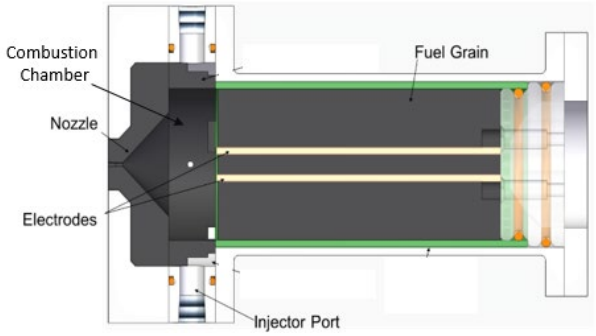

Figure 4. ASI End-Burn Configuration

"Sandwich" Motor Design

Similar to the end configuration, the "sandwich" configuration was designed to increase the flow of oxidizer across the fuel surface and to maintain a constant O/F ratio. The "sandwich" end burn motor was inspired by a design developed by Haag[16]. The combustion chamber is located between the two fuel grains, with one fuel grain bumping up against the nozzle and the other fuel grain containing the electrodes. Similar to the ASI end-burn configuration, the oxidizer is injected at eight points around the case wall to induce a swirling internal flow. The electrodes once again run through the length of the fuel grain and terminate flush with the combustion chamber surface allowing for fuel vaporization. A side view of the end burn design is shown in Figure 5. The intent of this approach was to minimize the area of the thruster case exposed to the combustion chamber with the goal of minimizing heat loss to the structure. The reduction in heat loss increased combustion efficiency and fuel packing efficiency beyond what was demonstrated by the ASI configuration.

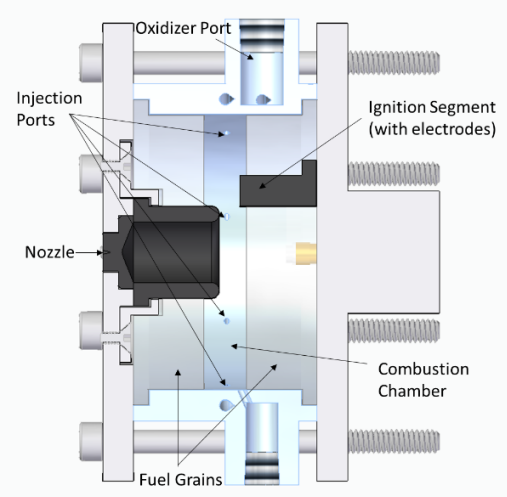

Figure 5. "Sandwich" End-Burn Configuration

Test Lab Hardware

The test cart used to test SDL's hybrid thruster is portable and can be wheeled from lab space to the testing area. It includes the necessary equipment to drive a gaseous oxygen (GOX) based hybrid motor, as well as a set of sensors and a data acquisition (DAQ) unit for characterizing the motor. A picture of the test cart is shown in Figure 6. A separate cart with the GSE control computer is shown in Figure 7, which is used to control thruster operation and data acquisition.

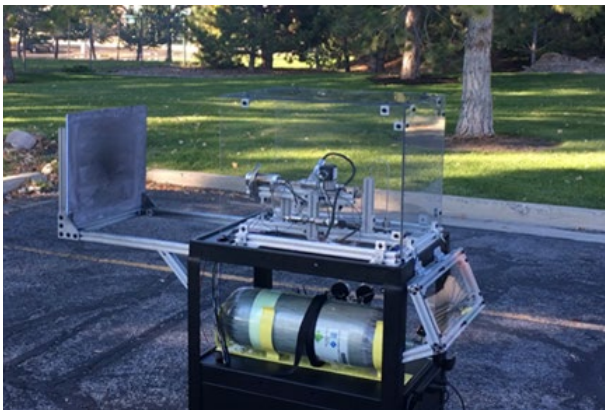

Figure 6. Portable Test Cart

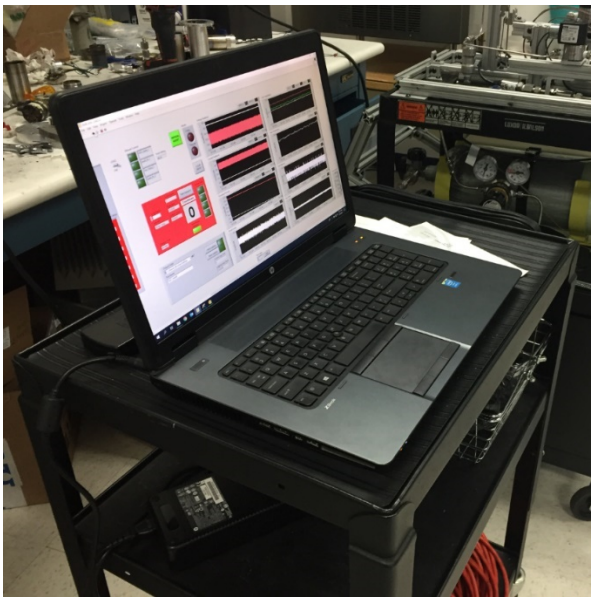

Figure 7. GSE Computer used to Test and Record Data

The sensors on the test cart are used to determine the performance of the motor and maintain a safe operating state. Temperature and pressure are measured for thruster characterization in addition to serving as a safety feature. The control software includes several user-set abort conditions to abort a test if an unsafe operating state is met, such as chamber pressure too high or nozzle temperature too high. Figure 8 below shows the sensors as mounted on the test cart.

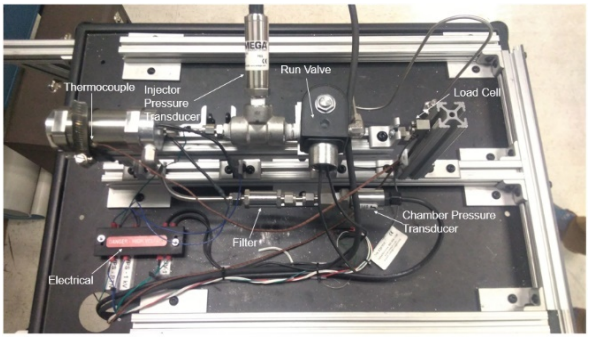

Figure 8. Thruster Mounted on Test Cart

The operational ranges of these sensors are shown in Table 1. The Test Cart DAQ unit has a resolution of 24 bits for load cells and thermocouples, and a resolution of 16 bits for all other channels. The DAQ unit is shown in Figure 9.

Table 1. Operating Ranges of Test Cart Sensors

Sensor	Operating Range
Chamber Pressure	0 – 300 psi
Injector Pressure	0 – 500 psi
Type J Thermocouple	0 – 482 ℃
Load Cell	0 – 22 N
Gas Flow Meter	0 – 80 LPM
Ignition Voltage	0 – 1100 V
Ignition Current	0 – 35 mA

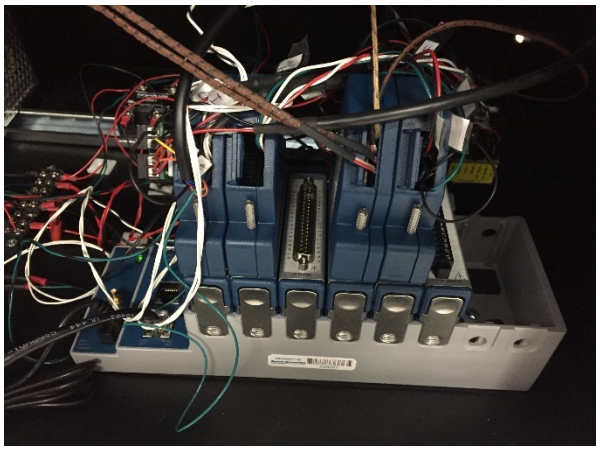

Figure 9. DAQ Unit Mounted inside Test Cart

Equipment to drive the motor consists of a pressure regulated GOX supply and a high-voltage power supply to drive the ignition system. The GOX valves and ignition system are powered separately through arming switches, giving each system a "safe" and "armed" state to eliminate the possibility of accidental ignition. This safety feature is shown in Figure 10.

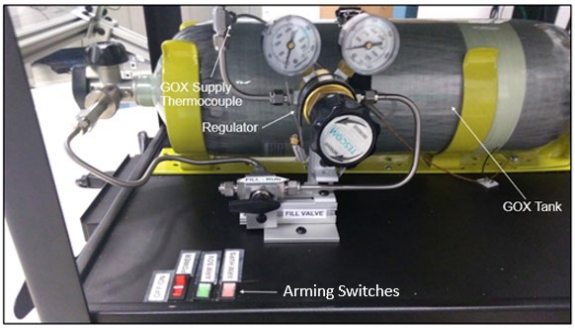

Figure 10. Middle Deck of the Test Cart

The thruster motor is mounted on an inverted pendulum thrust stand. This consists of Aluminum T-slot railing supported by three thin aluminum flexures. These flexures allow the structure to move in the direction of the thrust axis when the motor fires, resulting in load cell measurements. A computer-aided design (CAD) model of this mounting setup is shown in Figure 11.

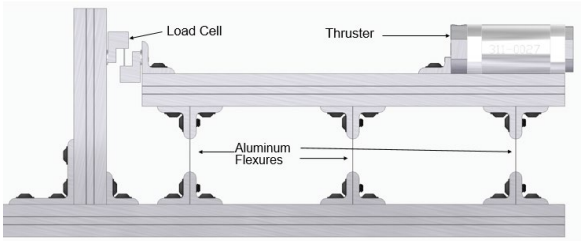

Figure 11 Motor Stand and Load Cell

There is a small amount of resistance to the movement of the motor mount due to the aluminum flexures and plumbing. To compensate, the load cell was calibrated while installed on the test cart with a pulley system to mimic a thrust event using calibrated weights.

In addition to single motor tests, the test cart has been configured to provide reaction control system (RCS) testing capabilities. A two-motor setup has been demonstrated on the test cart, and space exists to run a four-motor setup to simulate a full RCS control unit.

RESULTS AND DISCUSSION

ASI Test Results

An issue found during this testing campaign was the reliability of the arc ignition system. While using ABS as the fuel, the arc path was repeatedly covered with the vaporized but unburned fuel, leading to subsequent ignition failure. The unreliable ignition of ABS required an investigation into other plastics to use as the fuel, including Nylon-12, PMMA (Acrylic), and PVC. These fuels were selected based on an initial analysis using the NASA software package Chemical Equilibrium with Applications (CEA). The CEA analysis indicated favorable combustion properties over the use of ABS. Table 2 shows each fuel type and the key performance metrics used to select the final fuel.

Table 2. Fuel Grain Performance

Fuel Type	Average C* (m/s)	Average Rise time (sec)	Number of Ignitions observed
ABS	895	2.18	6
Nylon-12	860	2.56	17
PMMA	1022	1.86	30

ABS was the first fuel to be tested. The primary issue with ABS was the lack of repeatable ignitions. The motor had to be disassembled after each ignition to clean the carbon from the electrodes. Due to the low observed C* and the carbon present on the electrodes after a test, it was determined that the ABS combustion was incomplete.

Nylon-12 was used in several burns and was initially found to have better ignition reliability than ABS. However, the Nylon fuel would soften and flow during a test, which caused ignition failure and, in some cases, blocked the injector port. The regression rate in Nylon-12 was also found to have a major dependence on the bulk fuel temperature, leading to a long motor rise time as shown in Figure 12.

Testing with PVC revealed a significant material compatibility issue between the exhaust products and the graphite nozzle, leading to rapid nozzle erosion and failure. A single 15 second test would produce sparks in the exhaust plume and completely erode the throat of a new graphite nozzle. One afternoon of testing with PVC indicated that no further evaluation was required to determine its merit as a fuel.

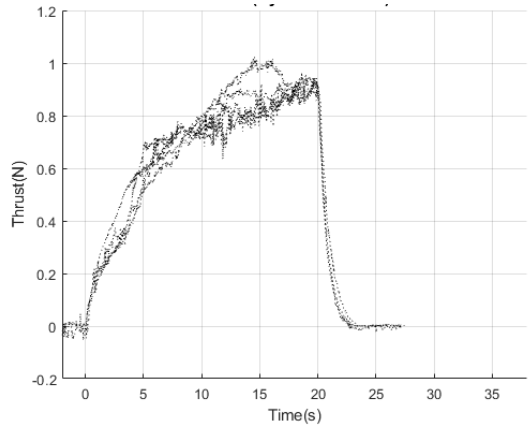

Figure 12. Thrust profile of 1 N End-Burn motor using GOX and Nylon 12

The final fuel studied was PMMA. PMMA exhibited a reduced regression rate as compared to ABS, and therefore had a reduced tendency to coat the electrodes in soot. Table 2 shows that PMMA had the greatest C*, which indicates a more efficient combustion process when compared to ABS and Nylon-12. Because of the reduced deposition of soot on the electrodes during each test, a greater number of consecutive ignitions was achieved. PMMA also has a higher melting point so it did not deform during extended duration burns. These favorable traits surrounding PMMA led to it being selected as the fuel for the majority of the testing campaign.

Testing the arc ignition system with these plastics found that ABS was the most reliable. The other plastics usually initiated an arc path but failed soon after in subsequent ignition attempts. This led to a common design of having a small segmented portion of the primary fuel grain containing ABS as the ignition system. This mitigated the above-mentioned ignition failure using only ABS. As a result, PMMA with an ABS ignition segment was the preferred motor configuration.

0.5 N and 1 N Test Firing Results

Two motors with different diameters of the ASI end-burning motor were tested. Figure 13 (a – f) shows the results from over twenty burns of the 4.1 cm diameter 0.5 N motor, while Figure 14 (a – f) shows the results from over twenty burns of the 7.5 cm diameter 1 N motor. The chamber pressure, thrust, and ignition power were directly measured by the test stand, while vacuum thrust was calculated from these and the measured oxidizer mass flow rates.

a) Measured Chamber Pressure

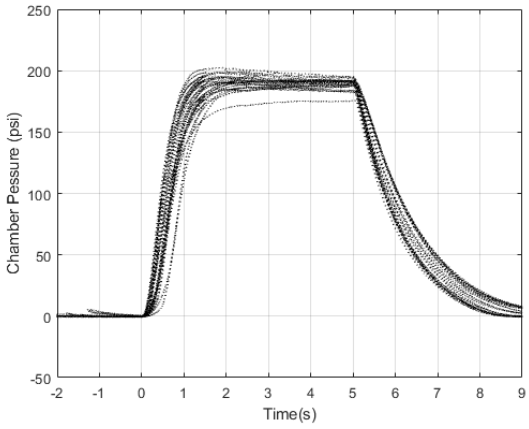

b) Ignition Power

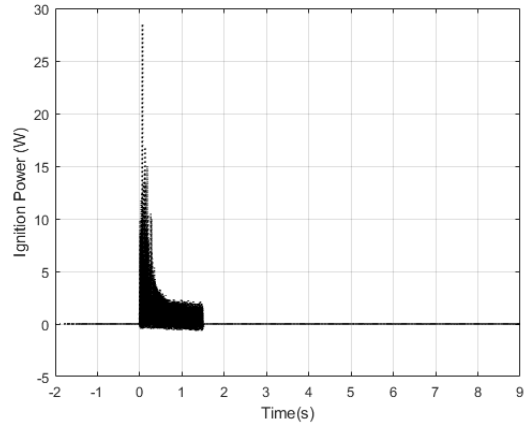

c) Measured Thrust

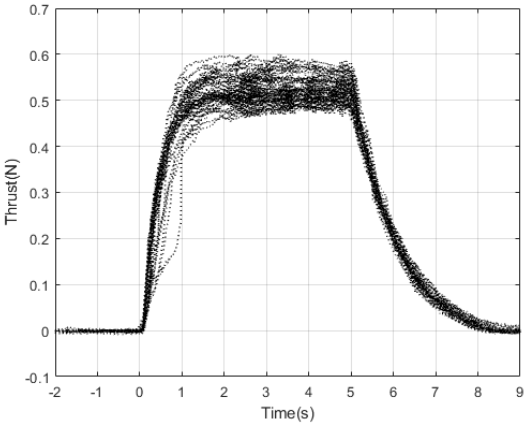

d) Extrapolated Vacuum Thrust

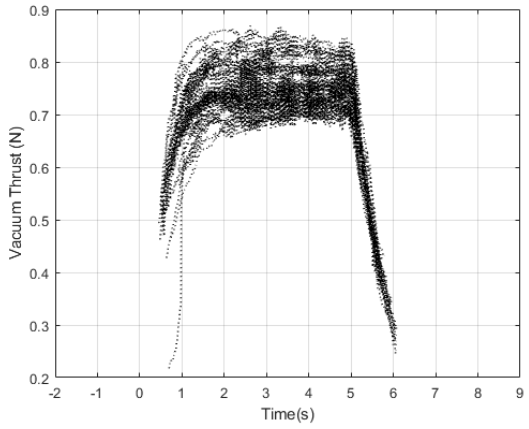

a) Measured Chamber Pressure

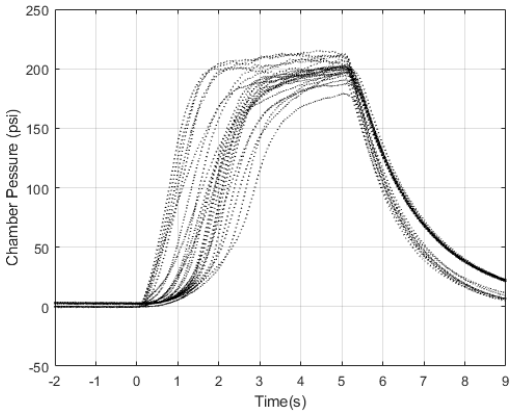

b) Ignition Power

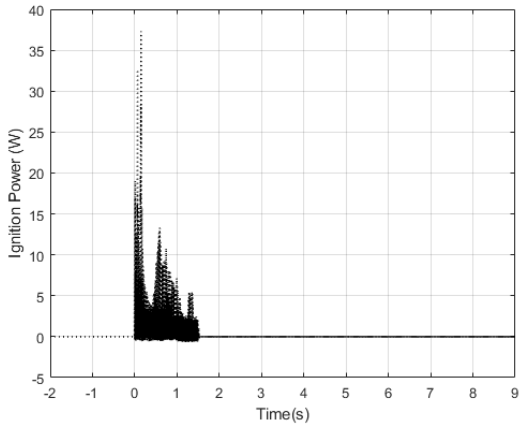

c) Measured Thrust

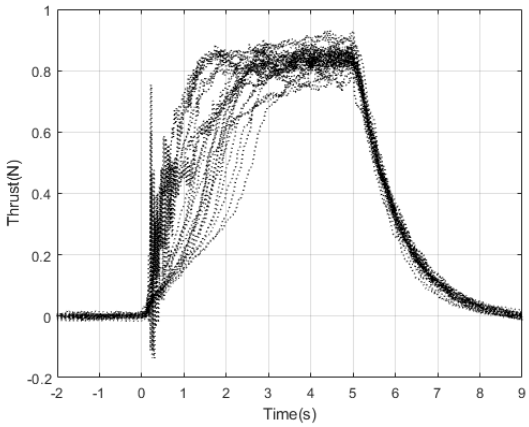

Figure 13. 0.5 N x 4.1 cm Diameter End-Burning Motor Test Data from twenty-seven 5-second burns with GOX and PMMA

d) Extrapolated Vacuum Thrust

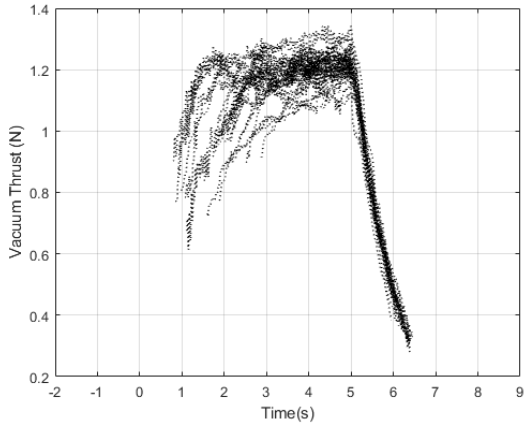

Figure 14. 1 N x 7.5 cm Diameter End Burning 1N Motor Test Data from twenty-seven 5-second burns with GOX and PMMA

Table 3 shows the calculated average I_{sp} and the extrapolated average Vacuum I_{sp} for each ASI end-burn configuration. The I_{sp} was calculated over the entire duration of the burn accounting for both the rise time and the tail-off time of the motor. The low I_{sp} of the ASI configurations is a direct result of an incorrect oxidizer-to-fuel ratio, which is controlled through both the geometry of the motors and the total injected oxidizer.

Table 3. I_{sp} for 4.1 cm and 7.5 cm End Burning Motors

Fuel Grain Diameter	Average Calculated Ambient I_{sp} (sec)	Average Extrapolated Vacuum I_{sp} (sec)
4.1 cm	115	162
7.5 cm	100	133

The ignition characteristics are similar for each test as shown in Figures 13 and 14. The chamber pressure, thrust, I_{sp} are not as similar between each burn, and vary widely. These performance variations relate to the variation in the oxidizer to fuel (O/F) ratio. Figure 15 shows the O/F ratio for each end burning motor diameter.

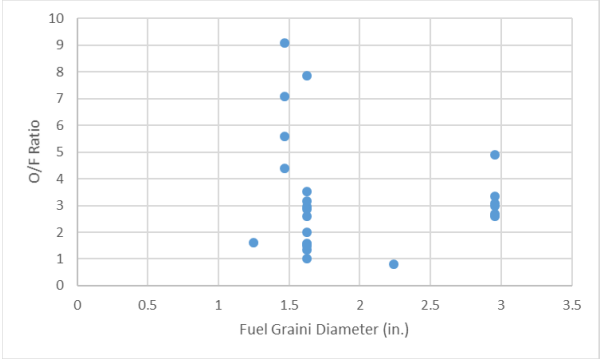

Figure 15. Comparison of O/F ratios at different fuel grain diameters

The O/F ratio tended to slightly increase with the diameter of the fuel grain. However, the overall inconsistencies in the O/F ratio and I_{sp} suggest that combustion is incomplete in these end burning configurations.

Core Burn vs. End-Burn Test Results

A comparison with a more traditional core burn configuration was completed. The core and end burning motors performed similarly to each other at the 1 N scale. A key difference is the change in the O/F ratio. The core burn motors were extremely fuel rich, while the end burning motors were oxidizer rich. The end burning motors were successful in producing a more constant burn area and thrust level during steady state when compared to the core burning motors. There was no notable difference in the I_{sp} between the core burn and end-burn configurations. Figure 16 (a – b) compares the thrust profiles of the core burn and end burn motors.

a) Core burn thrust

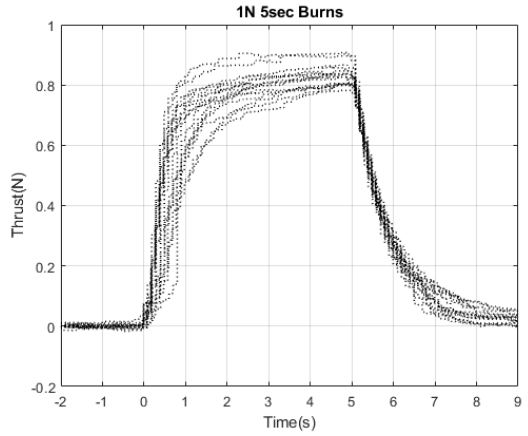

b) end-burn thrust

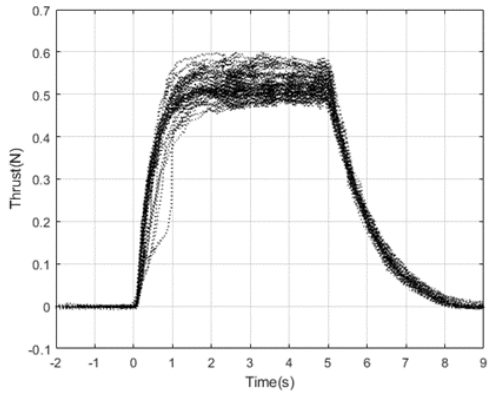

Figure 16. Comparison of thrust profiles of core burn (a) and end-burn (b) motors

Combustion Efficiency Analysis

During the testing campaign, it was discovered that a large amount of heat loss to the motor case occurred on a burn-to-burn basis. This heat loss directly stripped away from the combustion enthalpy, which explained much of the difference between the performance predicted by CEA and performance actually measured. Initial tests tracking the motor case temperature estimated that 20-40% of the enthalpy released in combustion was present as heat in the case at the end of a test, rather than being used to increase the chamber stagnation temperature. Two methods to try to mitigate this heat loss were developed and reached initial testing:

1. Insulate the case from the combustion chamber with a high temperature ceramic
2. Change to a "sandwich" geometry, with the combustion chamber located between two end-burn surfaces

Insulating the case brought the challenge of determining a suitable insulation material. Several ceramics were investigated with the common properties of withstanding high temperatures, resisting oxidizing environments, and having relatively low thermal conductivity. Some initial testing was done by modifying the end burn motors to include a ceramic insulator.

A "sandwich" end burn motor was also built and tested, derived from a design developed by Haag[16]. The intent of this approach was to minimize the area of the thruster case exposed to the combustion chamber and increase the fuel packing efficiency. Initial tests of this motor were promising showing an increase in I_{sp} by about 23% over an end-burn configuration of the same thrust level.

Figure 17 (a – d) shows the results from the sandwich motor testing campaign.

a) Measured chamber pressure

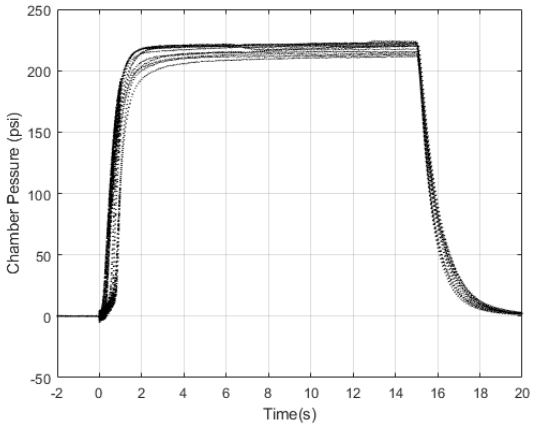

b) Ignition power

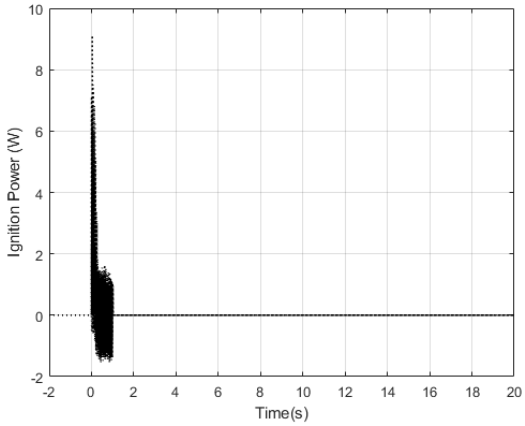

c) Measured thrust

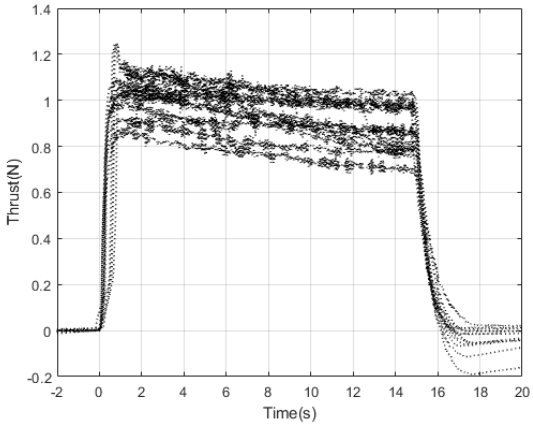

d) Extrapolated vacuum thrust

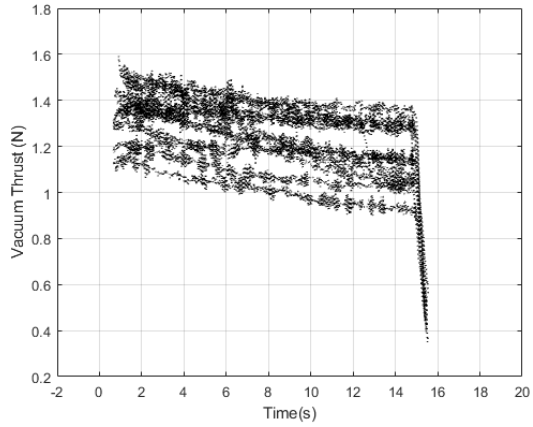

Figure 17. "Sandwich" configuration showing 13 x 15-second burns with GOX and PMMA

The heat present in the case was also reduced, averaging 12% of the combustion energy over the tests performed. The thrust rise time also improved from greater than 1-second (Figure 13a, Figure 14a) to ~350 msec. These changes also improved the ignition reliability. Table 4 shows the average calculated I_{sp} and the extrapolated vacuum I_{sp} for the "Sandwich" configuration. Again, the specific impulse was calculated over the total duration of the burn including the rise time and tail-off time of the motor.

Table 4. "Sandwich" End Burning Motor I_{sp}

Motor	**Average Calculated Ambient I_{sp} (sec)**	**Average Extrapolated Vacuum I_{sp} (sec)**
"Sandwich"	127	169

CONCLUSION

The propulsion laboratory at the Space Dynamics Laboratory recently finished testing of two hybrid rocket designs suitable for small satellites and CubeSats. This paper presents a novel idea of taking advantage of radiative heating, which traditionally had impeded the use of hybrid rockets as a propulsion system in the 1 N class. This paper presents the test results of two fuel grain designs, the first being an end-burning design and the second a "sandwich" fuel grain design. The analysis of various benign fuel grains paired with gaseous oxygen was presented. These systems are capable of producing a vacuum I_{sp} of greater than 150 seconds and a thruster rise time of less than 350 msec. Future investigations using high density oxidizers such as hydrogen peroxide and nitrous oxide are expected to further increase the performance of these end-burning hybrid motors beyond what was demonstrated in this paper

Acknowledgments

The authors would like to acknowledge Space Dynamics Laboratory for the funding of this project.

REFERENCES

1. Whitmore, S. A., Peterson, Z. W., and Eilers, S. D., "Comparing Hydroxyl Terminated Polybutadiene and Acrylonitrile Butadiene Styrene as Hybrid Rocket Fuels," *Journal of Propulsion and Power*, Vol. 29, No. 3, 2013, pp. 582-592. doi: 10.2514/1.B34382
2. Whitmore, S. A, Inkley, Nathan, and Merkley, Daniel P., "Development of a Power-Efficient, Restart-Capable Arc Ignitor for Hybrid Rockets", *Journal of Propulsion and Power*, Vol. 31, No. 6, 2015, pp. 1739-1749. doi: 10.2514/1.B35595
3. Sutton, George, P., and Biblarz, Oscar, *Rocket Propulsion Elements,* 8th Edition, 623 p.
4. Foust, J., "How big is the market for small launch vehicles?" April 11, 2016. Spacenews.com.
5. Iridium NEXT, "Hydrazine - Toxic for humans but satellits love it." June, 20, 2017, https://www.iridium.com/blog/2017/06/20/hydrazine-toxic-for-humans-but-satellites-love-it/
6. NASA, "State of the Art Small Spacecraft Technology", NASA/TP—2018–220027, Small Spacecraft Systems Virtual Institute, Ames Research Center, Moffit Field, CA.

7. Bulcher, A. M., & Whitmore, S. A. (2018). 'A green hybrid thruster using moderately enriched compressed air as the oxidizer." *2018 Joint Propulsion Conference*.

8. Anon., "Hazard Analysis of Commercial Space Transportation; Vol. 1: Operations, Vol. 2: Hazards, Vol. 3: Risk Analysis," U.S. Dept. of Transportation, Document PB93-199040, Accession No. 00620693, May 1988.

9. Foust, J., "Opportunities grow for smallsat rideshares launches". February 6, 2020. Spacenews.com

10. Chiaverini, M. J., Serin, N., Johnson, D. K., Lu, Y-C., Kuo, K. K., and Risha, G. A., "Regression Rate Behavior of Hybrid Rocket Solid Fuels," Journal of Propulsion and Power, Vol. 16, No. 1, Jan. 2000, pp. 125–132.

11. Anon. "Electromagnetic Environmental Effects Requirements for Systems". *Department of Defense Interface Standard*, *MIL-STD-46* December 2010.

12. Whitmore, S. A. (2018). Three-dimensional printing of "green" fuels for low-cost small spacecraft propulsion systems. *Journal of Spacecraft and Rockets*, *55*(1), 13–26. https://doi.org/10.2514/1.A33782

13. Whitmore, S. A., Merkely, D. P., & Inkley, N. R. (2014). "Power Efficient, Restart-Capable Acrylonitrile-Butadiene-Styrene Arc Ignitor for Hybrid Rockets." *Proceedings of the AIAA/USU Conference on Small Satellites*, 1–20.

14. Kuffel, E., Zaengl, W., and Kuffel, J., *High Voltage Engineering Fundamentals*, 2nd ed., Newnes Publishing, Oxford UK, 2000, Chapters. 5 & 6, pp. 281-394.

15. Merkley, S. L., "Effects of Radiation Heating on Additively Printed Hybrid Fuel Grain Oxidizer-to-fuel Ratio Shift" (2016). A*ll Graduate Theses and Dissertations*. Utah State University.

16. Haag, G. S., 2001. *Alternative Geometry Hybrid Rockets for Spacecraft Orbit Transfer*. Ph.D. University of Surrey